Coupled ENSO instabilities derived with breeding

Ming Cai and Eugenia Kalnay
Department of Meteorology, University of Maryland, College Park, MD 20742

This paper reports the ENSO instability properties derived from breeding experiments made with NASA NSIPP coupled GCM model. Bred vectors, the difference between a breeding run and the control run, are the naturally growing instabilities upon the evolving flow and are strongly related to forecast errors.

A 50-year control integration and two 10-year breeding experiments have been carried out using the NSIPP coupled model (1.25 by 2/3^o, 20 layers in the ocean and 3.75 by 3^o, 17 levels in atmosphere). Each of the two breeding experiments consists of 120 monthly integrations obtained by running the same executable file used for the control run, but with the control run restart files (initial conditions) to which we added a bred perturbation. We use as rescaling norm the rms of the SST difference between the control and perturbation run averaged over the tropical Pacific basin (15S-15N and 120-270) is used to measure the perturbation size (denoted as ***S***). The perturbation for each monthly integration has the same value of ***S*** equal to 0.085 ºC, about 10% of the SST variability over that area. The only difference between the two breeding runs is in the initial perturbation, which is determined from the differences between two randomly selected sets of restart files. Although the initial perturbations for the two breeding runs are substantially different in the ocean and especially in the atmosphere, the bred vectors generated by the two breeding runs have similar growth rates and spatial structures, implying the breeding method is indeed capable of capturing the fastest growing modes associated with background ENSO events.

The primary objective for these breeding runs is to assess whether it is feasible to separate the ENSO related coupled variability from the weather modes and other short time scale oceanic instabilities using the breeding technique. The results obtained with the Zebiak-Cane model (Cai et al. 2002) provide us with general guidelines for judging if the bred vectors obtained with the NSIPP model are those associated with ENSO-related coupled instability. Figure 1 shows monthly amplification rates derived from the two breeding runs with a reference to the evolution of the background ENSO events. The amplification rate of the bred vectors tends to be larger few month prior to or after a major extreme (warm/cold) event, in a good agreement with the results found in ZC model. The amplification rate is about 3 times as large as that found in the ZC model. The Niño-3 index of the bred vectors tends to have large amplitudes either before or after a major event (not shown). This again is consistent with the findings of the ZC model. The SOI indeces of the bred vectors show similar characteristics. Another feature is that the two breeding runs (BV1 and BV2) show virtually the same behavior, except that occasionally the sign of the bred vectors in the two breeding runs is opposite. This may be viewed as independent evidence showing the evolution of the bred vectors is strongly dictated by the background ENSO events. We have calculated three sets of regression maps against the Niño-3 index of the control run, and the Niño-3 index of the bred vectors derived from the BV1 and BV2 runs. As shown in Figure 2, there is some similarity between the regression maps of the tropical variables calculated from the control run and their counterparts from the breeding runs, although the latter tend to be narrower and have smaller scales, as in the ZC model. This suggests that dominant patterns captured in the breeding runs are ENSO-like perturbations at least within the tropical Pacific basin, as in the ZC model. Moreover, the similarity of the patterns derived from the two breeding runs suggests that despite the presence of large amplitude atmospheric noise, there is a still a single dominant ENSO instability, and that this leads to the robustness of the pattern captured by the bred vectors. The variability associated with the pattern shown in the regression maps explains more than 40% of total variability of the perturbation fields over the tropical Pacific basin in the breeding runs.

We have also calculated the regression maps of 500 hPa geopotential height of the control run and bred vectors derived from the two breeding runs (not shown). Again, we find that the regression maps of the BV1 and BV2 resemble each another. However, unlike the tropical response, the variability associated with the patterns only explains about 15% of the total perturbation variability over the globe in the breeding runs. Therefore, if we interpret the patterns shown in the regression maps to be associated with tropical ENSO variability, these signals are mixed with the background “weather noise” over the mid-latitudes. In other words, with the choice of ocean SST norm for rescaling, the breeding method is able to capture the ENSO-related instability over the tropical Pacific basin, but it cannot separate the remote

responses to the coupled tropical anomalies from the background weather noise over extratropics without using additional tools (such as the regression analysis). Since the breeding perturbations are associated with instabilities of the underlying flow and with forecast errors, we expect to be able to use these results within the data assimilation system and reduce the "errors of the month" within the analysis at low computational cost.

REFERENCES

Cai, M., E. Kalnay, and Z. Toth, 2002: Bred Vectors of the Zebiak-Cane Model and Their Application to ENSO Predictions. Accepted in J. Climate.

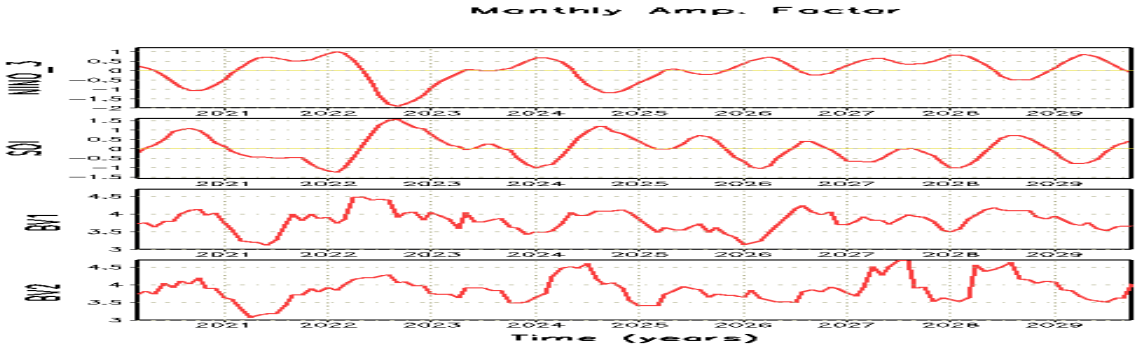

Figure 1. Monthly amplification factors of bred vectors of the NSIPP model. The top two panels are Niño-3 and SOI indexes of the background ENSO obtained from the control run. The bottom two panels are the monthly amplification factors of the two breeding runs.

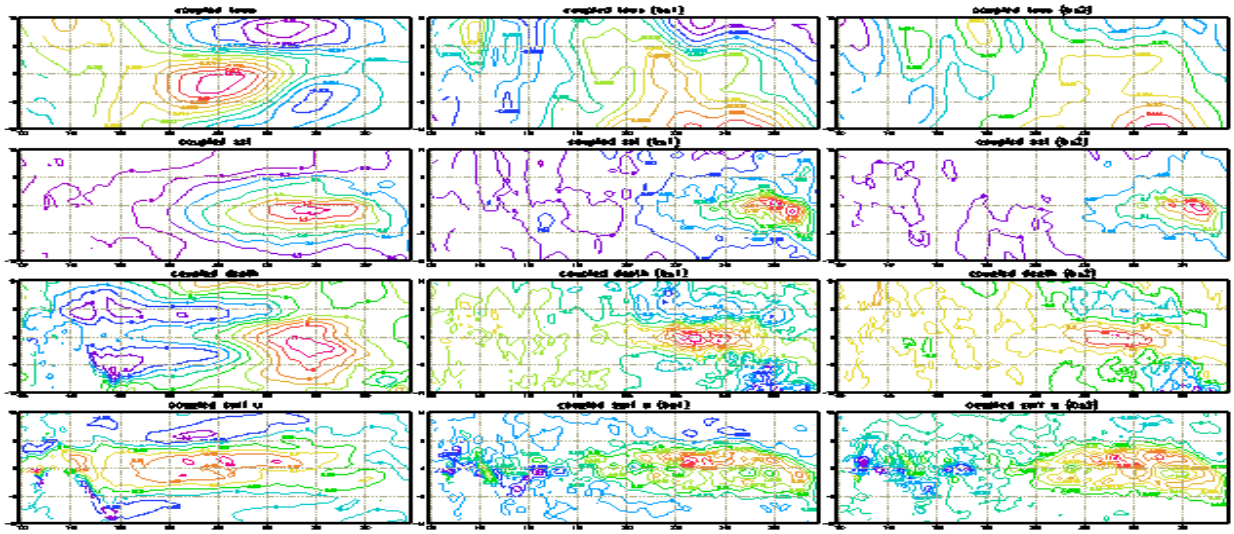

Figure 2. Regression maps of sample tropical variables (10S-10N) from the NSIPP model. The left panels are regression maps of the control run against the Niño-3 index of the control run, the middle panels are those of bred vectors derived from BV1 run against the Niño-3 index of the BV1 run, and the right panels are the same but for BV2. From the top to bottom, the variables are zonal wind stress, sea surface temperature, thermocline depth (the depth of the first seven layers), and surface zonal current.

On the coupling of a 3D Baltic Sea model to a regional atmospheric model

Ralf Döscher[1], Ulrika Willén, Colin Jones, Anna Rutgersson,
H.E. Markus Meier, Ulf Hansson and Phil Graham

Rossby Centre, Swedish Meteorological and Hydrological Institute (SMHI),
S-60176 Norrköping, Sweden

Regional coupled ocean-atmosphere-ice-landsurface models represent a major element on the way to assess the energy budget and water cycle over the Baltic Sea catchment area and to understand interaction across interfaces. To approach that goal, coupled regional models with the capability to run decades need to be developed and verified. This is currently done at the Rossby Centre within the Swedish Meteorological and Hydrological Institute (SMHI) for a northern European domain including the Baltic Sea (Fig. 1). The Rossby Centre Atmosphere Ocean model RCAO has been developed within the framework of the Swedish Regional Climate Modeling Program (SWECLIM) in order to perform downscaling of global climate scenarios and nowtime data. The latter is in accord with the goals of the GEWEX subprogram BALTEX. A description of the coupling and first evaluation of fluxes is given by Döscher et al. (2002). Meier and Döscher (2002) give a description of Baltic Sea flux budgets.

The interactively coupled ocean within RCAO is limited to the Baltic Sea. The remaining ocean areas are represented by a one-way data transfer of sea surface quantities to the atmosphere. The component models of RCAO are the Rossby Centre models for ocean (RCO, including sea ice) and atmosphere (RCA, including land surface). RCO is a 3D ocean model described by Meier al. (2002). RCA is described in detail by Rummukainen et al. (2001) and Jones et al. (2001). River runoff to the Baltic Sea is represented by a river routing scheme connecting the land runoff with river mouths. RCAO features a resolution of 44 km for the atmosphere and 6 nautical miles for the ocean. The coupling interval is 30 minutes. The ocean and atmosphere models are interactively coupled via the OASIS coupler (Valcke et al., 2000). The coupled system is parallel which enables efficient integrations on climate related timescales.

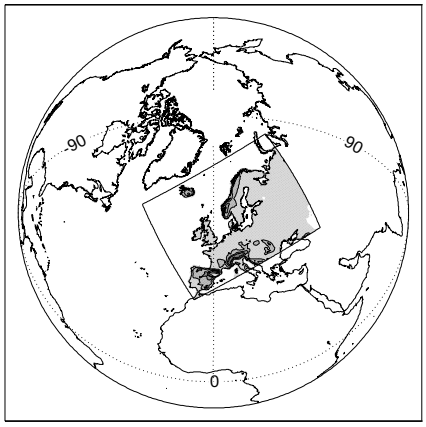

Figure 1: RCAO model domain for hindcast runs, covering most of Europe and parts of the North Atlantic Ocean and Nordic Seas. Only the Baltic Sea is interactively coupled.

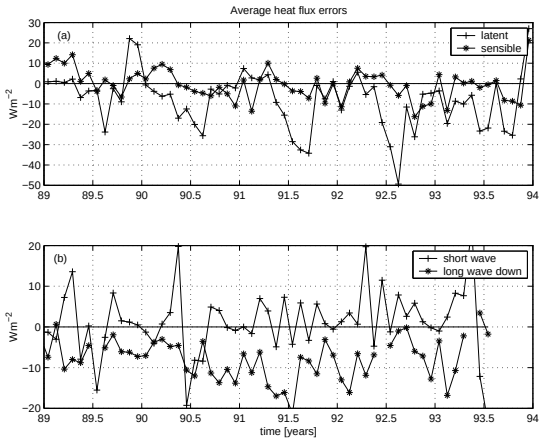

Figure 2: Heat flux errors. (a): latent/sensible heat flux over the Baltic - observation (daSilva), (b): shortwave/longwave heat flux over land - observation (SMHI station data)

A validation of RCAO is carried out by comparing 5-year long coupled hind-cast runs with observations and an ocean stand-alone run. The coupled system is forced with ECMWF reanalysis data (ERA15) at the atmosphere's lateral boundaries. The system does not use flux corrections. The coupled sea surface temperature (SST) matches observations well for five years in a row. SST's are statistically equivalent

[1]Corresponding author's email: ralf.doescher@smhi.se

to the uncoupled ocean model forced by observations (Mean error amplitude is close to 0.3 K for both). Despite this statistical similarity, differences occur contributing to an overestimation of sea ice extent throughout the winters in the coupled ocean. The ice area is especially overestimated during strong winters. This problem can be related to incorrect fluxes before and during winter. Negative biases are seen in the latent heat fluxes over sea and in downward longwave radiation (Fig. 2) The latent heat flux differs from observations by up to 50 Wm^{-2}. Largest differences are negative and occur during late summer and fall. Thus, the coupled ocean loses too much heat before the beginning of the ice period. The surface turbulent fluxes of sensible and latent heat in the RCA-model are calculated using mean model parameters and transfer coefficients as described by Rutgersson et al. (2001), modified by Makin and Perov (1997). Our results show that further improvement is needed for the latent heat flux, while sensible heat flux of the coupled run fits well with observations. Fig. 2b shows a good agreement of model and observation regarding shortwave radiation. The longwave downward radiation shows a clear negative bias, thus leading to the overestimation of sea ice. Newer model runs indicate that the negative bias disappears on longer timescales. The atmospheric formulation of the surface long-wave downward radiation depends on assumptions about the vertical overlap of clouds in a grid column. "maximum overlap" (Savijärvi 1990) is used in our coupled run. A more physically based assumption, "maximum-random overlap" (Weare 2001), was tested in an additional coupled run. This gives better wintertime SST's and sea-ice extent, since the effective cloud cover was increased leading to increased long-wave radiation towards the surface and a reduced long-wave surface bias. However, a summertime warm bias became worse. The stability of the coupled ocean's surface temperature appears robust on the annual timescale. Flux errors of the magnitude discussed above are always compensated by the response of SST and accordingly adjusted fluxes. In the 5-year mean, the total heat content of coupled and uncoupled ocean are similar within 4% without a trend. In that sense, the coupled system is free of drift. Thus, the coupled system is suitable for multi-year runs. The ocean surface elevation variability is significantly more realistic for stand-alone ocean runs.

We conclude that the coupled model performance is good with respect to most fluxes and longterm stability. However, a coupled forcing for the ocean model cannot completely replace observation-based forcing for hind-cast runs. For longer forecast and scenario runs, of course, the atmosphere model provides the only possible forcing. A 3D Baltic Sea ocean model as RCO provides the best currently possible lower boundary condition for the coupled regional atmosphere in hind-cast mode, as it provides high resolution for surface quantities in good quality. This is not available from observations. This is even more true for longterm forecast runs as sea surface quantities can only be delivered by an ocean model. Future work needs to address the issues of latent and longwave heat flux. Moreover, a more detailed evaluation for longer simulation periods is planned. Further, interaction of sub-basin scale ocean processes with ocean-atmosphere fluxes will be examined.

References

Döscher R., Willen U., Jones J., Rutgersson A., Meier H.E.M. & Hansson U 2002: The development of the coupled ocean-atmosphere model RCAO. *Boreal Env. Res.*, submitted.

Jones C. 2001: A brief description of RCA2. *SWECLIM Newsletter* 11, November, 9-14.

Makin V. K. & Perov V. 1997: On the Wind Speed Dependence of Momentum, Sensible Heat and Moisture Exchange Coefficients Over Sea in the HIRLAM Model-a case study, *Hirlam Newsletter*, 29, pages 26-31. SMHI, SE-601 76 Norrköping, Sweden.

Meier H.E.M., Döscher R. & Faxén T. 2002: A multiprocessor coupled ice-ocean model for the Baltic Sea: application to salt inflow. *J. Geophys. Res.*, submitted.

Meier H.E.M. & Döscher R. 2002: Simulated water and heat cycles of the Baltic Sea using a 3D coupled atmosphere-ice-ocean model. *Boreal Env. Res.*, submitted.

Rummukainen M., Räisänen J., Bringfelt B., Ullerstig A., Omstedt A., Willén U., Hansson U. & Jones C. 2001: A regional climate model for northern Europe: model description and results from the downscaling of two GCM control simulations. *Clim. Dyn.*, 17: 339-359.

Rutgersson A., Smedman A.-S. & Omstedt A. 2001: Measured and simulated latent and sensible heat fluxes at two marine sites in the Baltic Sea, *Bound.-Layer Meteor.*, 99, 53-84.

Savijärvi H. 1990: Fast radiation parametrization schemes for mesoscale and short-range forecast models. *J. Appl. Meteor.*, 29, 437-447.

Valcke S., Terray L., and & Piacentini A., 2000: Oasis 2.4, Ocean atmosphere sea ice soil: user's guide. *Technical Report TR/CMGC/00/10*, CERFACS, Toulouse, France, 58 pp.

Weare B.C. 1989: Effects on cloud overlap on radiative feedbacks. *Clim. Dyn.*, 17, 143-150.

An Assessment of Natural Variations in the Thermohaline Circulation and Climate Using a 1400 Year Coupled Model Calculation

Jeff Knight, Rob Allan, Chris Folland and Michael Vellinga

Hadley Centre, Met Office, London Road, Bracknell, Berkshire, United Kingdom

email: jeff.knight@metoffice.com

Results from a 1400 year calculation using the HadCM3 coupled climate model without external forcings are show the existence of a quasi-periodic mode of internal climate variability with a characteristic time scale of about 100 years. This mode is manifest in the modelled thermohaline circulation (THC), defined as the peak meridional overturning streamfunction at 30°N, which shows multi-decadal variations in strength of about 2 Sv (10%) with a coherent phase evolution for periods of up to 50 years. Additionally, global and northern hemisphere mean surface temperatures are found to vary in phase with the THC, with regressions of 0.05°C Sv^{-1} and 0.09°C Sv^{-1} respectively, suggesting that the mode is significant compared with twentieth-century climate variability. An influence on surface temperature in broad regions of the northern hemisphere is found, particularly in the North Atlantic, Pacific and Asia, as well as wind and rainfall effects, notably in Europe, north-east Brazil and the Sahel.

In the natural climate system, a lack of sub-surface marine monitoring prevents knowledge of possible past fluctuations in THC strength, constraining us to use coupled ocean-atmosphere models to make inferences about its potential behaviour. Model relationships between the THC and sea surface temperature (SST) are used to infer the strength of the natural THC and its role in the climate variability of the instrumental period. We find in particular that an increase in the THC would be consistent with a significant part of early twentieth century warming. In recent decades, SST changes similar to those observed are shown to be consistent with THC strengthening in the model. We also note the possibility that THC-climate relationships imply that the degree of future global climate warming could be temporarily enhanced or offset.

Regional regimes with drought and extreme wet conditions: Possible changes in XXI century from IPSL-CM2 simulations

I.I. Mokhov, J.-L. Dufresne, V.Ch. Khon, H. Le Treut, V.A. Tikhonov

Obukhov Institute of Atmospheric Physics RAS, Moscow, Russia
Laboratoire Meteorologie Dynamique du CNRS, Paris, France

In this study we analyse possible regional changes of drought and extreme wet conditions in the XXI century relative XX century from simulations of a coupled atmosphere-ocean general circulation model (AOGCM) IPSL-CM2 with a carbon cycle for the 1860-2100 period (Friedlingstein et al., 2001; Dufresne et al., 2002). The IPSL-CM2 includes the LMD-5.3 AGCM (Le Treut and Li, 1991), the OPA-ice OGCM (Delecluse et al., 1993) and the OASIS coupleur (Terray et al., 1995). The carbon model includes the SLAVE code (Friedlingstein et al., 1995; Ciais et al., 1999) for the terrestrial part and the the IPSL-OGCM1 code (Aumont et al., 1999), based on the HAMOCC3 biochemical scheme (Maier-Reimer, 1993) for the ocean part. The scenario with the carbon dioxide emissions due to fossil and land use from observations up to 1990 (Andres et al., 1996) and the IPCC SRES98-A2 emission scenario from 1990 to 2100 (Nakicenovic et al., 2000) in these simulations were used.

There are different characteristics of drought and wet regimes. In particular, we analyzed model simulations of extremal meteorological conditions in May-July for the basic cereals-producing regions in the eastern European (EEP) and western Asian (WAP) parts of the former Soviet Union in comparison with observations from (Meshcherskaya and Blazhevich, 1997) for 1891-1995. In this case, for instance, the index D characterized the drought conditions with the negative precipitation anomalies ΔPr (normalized on the long-term mean value, MV, of precipitation) larger than -20% and positive temperature anomalies ΔT larger than 1K. The index W characterized the wet conditions with $\Delta Pr>20\%$ and $\Delta T<-1K$. Two additional indices were also analyzed: D-W and $S=(\Delta T/\sigma_{\Delta T} - \Delta P/\sigma_{\Delta P})$, where $\sigma_{\Delta T}$ and $\sigma_{\Delta P}$ are respective standard deviations (SD).

There is a quite good agreement between model simulations and observations for SD of ΔPr (± 0.16 and ± 0.15) and for MV and SD of ΔT ($0\pm 1.3^{o}C$ and $1.0\pm 1.0^{o}C$) in the EEP. There is also good agreement in the WAP for MV of ΔT ($0^{o}C$ and $0^{o}C$) with a larger deviations for respective SD ($0\pm 1.4^{o}C$ and $0\pm 0.9^{o}C$) and for SD of ΔPr (± 0.10 and ± 0.17).

Model simulations reproduce quite well the dependence of ΔPr on ΔT for EEP ($dPr/dT = -0.06\pm 0.01^{o}C^{-1}$ with coefficient of correlation r=0.47, while from observations $dPr/dT = -0.07 \pm 0.01^{o}C^{-1}$, r=0.52) for the period 1891-1995. The reproduction of this dependence for WAP is not so well (from observations $dPr/dT = -0.11\pm 0.02^{o}C^{-1}$ with r=0.58, while no significant relation was found from model results).

Table 1 shows changes of different characteristics in summer between XXI and XX centuries from model simulations for East (EER: 46.1-53.2 ^{o}N, 39.4-50.6 ^{o}E) and West (WER: 46.1-53.2 ^{o}N, 0-11.2 ^{o}E) European regions. The D and M values characterize the portions (%) of total area under corresponding conditions during summer months. According to Table 1 model results display that the increase of temperature in the XXI century is accompanied in both regions by the decrease of precipitation and M and by the increase of D, D-M and S. It should be noted that changes in EER are not statistically significant. The appropriate changes in WER are more remarkable. Model simulations show the SD increase (in brackets) in the XXI century for temperature in both regions and for precipitation in WER, while the SD decrease for precipitation in EER. The drought indices display the general SD increase, while the wet conditions index M shows the SD decrease.

This work was supported by the CNRS/RAS Program and by the Russian Foundation for Basic Research.

Table 1.

Region	Century	T,°C	Pr	D, %	M, %	DM, %	S
EER	XX	0 (± 1.2)	1 (± 0.2)	3.6 (± 8.1)	3.0 (± 7.5)	0.6 (± 11.6)	0 (± 1.0)
	XXI	2.2 (± 1.5)	0.9 (± 0.2)	12.5 (± 13.1)	0.3 (± 2.0)	12.3 (± 13.5)	1.4 (± 1.0)
WER	XX	0 (± 0.9)	1 (± 0.1)	3.2 (± 6.4)	1.3 (± 4.5)	1.9 (± 8.0)	0 (± 0.7)
	XXI	2.9 (± 1.5)	0.8 (± 0.2)	30.2 (± 19.4)	0	30.2 (± 19.4)	2.4 (± 1.3)

References

1. Friedlingstein P., L. Bopp, P. Ciais, J.-L Dufresne, L. Fairhead, H. LeTreut, P. Monfray, and J. Orr, 2001: Positive feedback between future climate change and the carbon cycle. Geophys. Res. Lett. V.28. No.8. P.1543-1546.
2. Dufresne J.-L., P. Friedlingstein, M. Berthelot, L. Bopp, P. Ciais, L. Fairhead, H. LeTreut, P. Monfray, J. Orr, 2002: Direct and indirect effects of future climate change on land and ocean carbon. Geophys. Res. Lett.
3. Meshcherskaya A.V., and V.G. Blazhevich, 1997: The drought and excessive moisture indices in a historical perspective in the principal grain-producing regions of the Former Soviet Union. J. Climate. V.10. P.2670-2682.
4. Le Treut, H., and Z.X. Li, 1991: Sensitivity of an atmospheric general circulation model to prescribed SST changes: feedback effects associated with the simulation of cloud optical properties. Clim. Dyn., **5**, 175-187.
5. Delecluse, P., G. Madec, M. Imbard, and C. Levy, 1993: OPA version 7, Ocean General Circulation Model, Reference Manual., Tech. Rep., IPSL.
6. Terray, L., E. Sevault, E. Guilyardi, and O. Thual, 1995: The OASIS Coupler User Guide Version 2.0., Tech. Rep., CERFACS TR/CMGC/95-46.
7. Friedlingstein, P., I. Fung, E. Holland, et al., 1995: On the contribution of CO_2 fertilization to the missing biospheric sink. Glob. Biogeochem. Cycles, **9**, 541-556.
8. Ciais, P., P. Friedlingstein, D. Shimel, and P. Tans, 1999: A global calculation of the dC of soil respired carbon: Implications for the biospheric uptake of anthropogenic CO_2. Glob. Biogeochem. Cycles, **13**, 519-530.
9. Aumont, O., J. Orr, P. Monfray, G. Madec, and E. Maier-Reimer, 1999: Nutrient trapping in the equatorial Pacific: The ocean circulation solution. Glob. Biogeochem. Cycles, **13**, 351-369.
10. Maier-Reimer, E.,1993: Transport and storage of CO_2 in the ocean - an inorganic ocean-circulation carbon model. Glob. Biogeochem. Cycles, **7**, 645-677.
11. Andres, R., G. Marland, I. Fung, and E. Matthews, 1996: A 1^o x 1^o of carbon dioxide emissions from fossil fuel consumption and cement manufacture, 1950-1990. Glob. Biogeochem. Cycles, **10**, 419-429.
12. Nakicenovic, N., J. Alcamo, G. Davis, et al., 2000: IPCC Special Report on Emissions Scenarios. Cambridge University Press, Cambridge, United Kingdom and New York, NY, USA, 599 pp.

Recent Developments in RPN Coupled Numerical Modelling

Harold Ritchie[1,2], Pierre Pellerin[1], and Serge Desjardins[2]

[1]Meteorological Service of Canada, Recherche en prévision numérique, Dorval, QC H9P 1J3
[2]Meteorological Service of Canada - Atlantic Region, Dartmouth NS B2Y 2N6
Corresponding author e-mail: Harold.Ritchie@ec.gc.ca

The coupled numerical modelling group at Recherche en prévision numérique (RPN) is supporting research and development for environmental prediction based on coupling a variety of numerical prediction models. Much of this is being accomplished through the Atlantic Environmental Prediction Research Initiative (AEPRI) in Halifax, Nova Scotia, in collaboration with other government, industry, and academic partners. Significant progress has been made in projects particularly in collaboration with the Meteorological Service of Canada (MSC) - Atlantic, the Oceanography Department of Dalhousie University (Dal), and l'Institut Maurice-Lamontagne (IML) in Mont-Joli Québec. The main ongoing coupled modelling and AEPRI sub-projects are: atmosphere-ocean coupling via the NSERC/MARTEC/MSC Industrial Research Chair in "Regional Ocean Modelling and Prediction" in the Oceanography Department at Dal, coupling data assimilation and prediction systems for coastal applications, modelling the extratropical transition of hurricanes and typhoons (e.g., Ma et al., 2002), coupled atmosphere-wave models, coupled atmosphere/land-surface/hydrology models, coupling with estuary models, and developing expert systems for marine applications. Numerous Environment Canada (EC) scientists have gained valuable experience and made significant progress in projects in the areas of storm surge prediction, improved oil spill trajectory modelling, wave modelling, severe weather prediction, and streamflow prediction, including preparing some new and innovative forecast products which have been implemented.

In particular, a storm surge prediction system, in which the Dal coastal ocean model is driven by operational regional forecast model surface pressure and wind fields, was successfully tested in experimental mode at MSC-A (Bobanovic et al., 2002). Subsequently an operational storm surge prediction and alert system was transferred and implemented in the Maritimes Weather Centre in December 2000 and the Newfoundland Weather centre in January 2001. The alert portion notifies the duty forecasters of potential storm surge events. Based on the model output, NWP guidance, and observations, the duty forecaster may issue an advisory or a warning message for storm surge. The system proved effective several times since its implementation and has helped protect life and property during storm surge events. The storm surge prediction system has also been used to examine the increasing probabilities of flooding due to storm surge in a changing climate. This is part of a Climate Change Action Fund (CCAF) project in which AEPRI is playing a key role. The probable maximum storm methodology has been applied to the January 21, 2000 storm surge case, and the results have been diagnosed and included in the CCAF project report (Thompson et al., 2002).

The St. Lawrence Estuary is a relatively well observed and physically convenient "test-bed" for calibrating and validating many of the components of the environmental prediction system that is being developed. A related project at IML is entitled "Gulf of St. Lawrence Ice-Ocean-Atmosphere Climate Change, Detection and Impact on the Canadian Energy Sector". Through this collaboration we are helping improve the active coupling between atmosphere and ocean models and improve forecasts for maritime transport, search and rescue, and environmental emergencies. Following an initial study (Saucier et al., 2002) atmosphere, ocean and ice models are now completely coupled in a two-way interactive system. Experiments have demonstrated a significant positive impact of the interactions on the atmospheric precipitation and temperature forecasts in winter.

In another collaboration with IML entitled "Modèles atmosphérique et hydrologique couplés à l'échelle régionale: Région des lacs des Deux-Montagnes et Saint-Louis", an atmosphere-hydrology coupled modelling system has been validated on a 30-day period. This system consists of a distributed hydrological model (WATFLOOD 1 km), radar data (1 km), atmospheric model (35 km, 10 km and 3 km) and the IML hydrodynamic model. The first validation covers the hydrological basins contributing to the St. Lawrence River between Lachine and the Cornwall dam, Lac des Deux Montagnes, Lac St. Louis, and the Milles-Iles and des Prairies rivers between the St. Lawrence River and the Carillon dam (Outaouais River). This coupled modelling system is being used to improve radar data (collaboration with McGill University), to calibrate the hydrodynamic model (collaboration with IML), to prepare a system for forecasting the water level of the St. Lawrence River (collaboration with IML), and to validate and improve atmospheric model predictions.

AEPRI is becoming even more inter-disciplinary and is integrating activities amongst EC`s various sectors. For example, the SLICK oil spill model is being used to give support to a project to study birds oiled at sea, and the AEPRI partners are principal investigators in further projects on the prediction and mitigation of coastal flooding, as well as for a coupled atmosphere /ocean / biological / optical observing and prediction system to study pollution in coastal inlets. In this research project Dalhousie University, together with MSC and other partners, is developing the ability to observe and forecast physical, optical, and biological changes in the marine environment. Acquisition and construction of instrumentation are in progress for the coastal embayment component of this Marine Environmental Prediction System, and initial deployment is anticipated this spring in Lunenburg Bay, Nova Scotia.

Through this series of mutually beneficial collaborative research and development projects, partners are effectively leveraging limited resources to produce innovative and practical environmental prediction tools and products.

References

Bobanovic, J., K.R. Thompson, S. Desjardins and H. Ritchie, 2002: Forecasting Storm Surges along the East Coast of Canada and Northeastern U. S. for the 21 January 2000 Storm. *Mon. Wea. Rev*., submitted.

Ma, S., H. Ritchie, J. Gyakum, J. Abraham, C. Fogarty and R. McTaggart-Cowan, 2002: A Study of the Extra-Tropical Re-Intensification of former Hurricane Earl using Canadian Meteorological Centre Regional Analyses and Ensemble Forecasts. *Mon. Wea. Rev*., conditionally accepted.

Saucier, F.J., F. Roy, D. Gilbert, P. Pellerin and H. Ritchie, 2002: The Formation and Circulation Processes of Water Masses and Sea Ice in the Gulf of St. Lawrence. *J. Geophys. Res*., accepted.

Thompson, K., H. Ritchie, N. Bernier, J. Bobanovic, S. Desjardins, P. Pellerin, W. Blanchard, B. Smith and G. Parkes, 2002: Modelling Storm Surges and Flooding Risk at Charlottetown. Appendix 2, Report on Climate Change Action Fund project CCAF A041 - Coastal Impacts of Climate Change and Sea-Level Rise on Prince Edward Island.

IMPLEMENTATION OF THE JMA TYPHOON MODEL COUPLED WITH THE MRI MIXED LAYER OCEAN MODEL AND ITS APPLICATION FOR TYPHOON BILIS

Akiyoshi Wada[1*] and Hiroshi Mino[2]
[1]Meteorological Research Institute, Tsukuba, Ibaraki, Japan
[2]Forecast Division, Japan Meteorological Agency, Tokyo, Japan
[1]awada@mri-jma.go.jp

1. Introduction

We, JMA (Japan Meteorological Agency)/MRI(Meteorological Research Institute) are developing a numerical weather prediction model coupled with a mixed layer ocean model (typhoon-ocean coupled model) in order to improve mainly forecasts of the intensity of tropical cyclones (TCs). The JMA typhoon Model (TYM) updated on March 2001 is an operational regional model with an initialization technique for TC (typhoon bogusing). The MRI mixed layer ocean model is designed according to appendix of Bender et al.(1993) and is developed by Wada (2002). The typhoon-ocean coupled model is based on the combination of these two models. Here, the impact on which the spatial distribution of SST and the SST variation affect the prediction of intensities of Typhoon Bilis is investigated.

2. Procedure of the typhoon-ocean coupled model, and initial and boundary conditions

The exchange process between the atmosphere and the ocean in the typhoon-ocean coupled model is explained. Some physical elements are exchanged between the atmosphere and the ocean whenever the ocean model runs one time step because the ocean model generally adopts a longer time step than that of the TYM. The physical elements of the TYM handed over to the ocean model are wind stresses, sensible and latent heat fluxes, and the information of topography used in the TYM. The effect of long-wave radiative heat flux and solar insolation is neglected in this typhoon-ocean coupled model. The direction of wind stresses can be modified when the TYM adopts Lambert coordinate system. As for the exchange methodology at the atmosphere-ocean interface, all elements handed over to the ocean model are all linearly interpolated to the coordinate system of the ocean model. The horizontal grid resolution of the TYM is 24km around the typhoon center and 1/5 degrees of the ocean model. The ocean model can be executed in one step after these procedures. The model-computed SST is then given to the TYM after the linear interpolation like the exchange from the atmosphere to the ocean. With regard to the ocean initial conditions of sea temperatures and salinities, Levitus climatological data are given, however initial SSTs are derived from the TYM at the initial time. The atmospheric initial conditions are usually determined from the objective analysis system in JMA Global spectral model (GSM). However, the atmospheric initial conditions are obtained from the predictions of the GSM at T+00h in this experiment. The atmospheric boundary conditions determined by GSM are applied every 3 hours.

3. Impact on which SST cooling affects the intensities of Typhoon Bilis

First, we conducted two numerical experiments using the TYM with two SST data, the climate SST and the daily SST, in order to investigate the prediction difference of the intensities of TCs in the different spatial distribution of SST. We took the case of Typhoon Bilis on August 20, 2000 for example, which the initial time of this simulation was at 1200 UTC 20 August 2000. Both experiments indicated the developing of Typhoon Bilis. The central pressure of Typhoon Bilis was 933.3hPa in the climate SST and 920hPa in the daily SST after T+39h (Figure 1). The difference of 13.3hPa was largely because the daily SST was 1 degree greater than the climate SST along the typhoon translation.

Next, we compared the TYM with the typhoon-ocean coupled model using the daily SST. The central pressure of Typhoon Bilis was 925.2hPa after T+39h (Figure 1) in the typhoon-ocean coupled model. The difference of the intensity of Typhoon Bilis between the TYM and the typhoon-ocean coupled model was 5.2hPa and less than the difference in between the climate SST and the daily SST. According to the result of the typhoon-ocean coupled model, Maximum SST cooling was about 1.4 ℃ (Figure 2) that was smaller than the SST by TRMM/TMI (Figure 3).

As noted the atmospheric responses, the effect of the negative feedback can be seen from the result of the typhoon-ocean coupled model. A maximum wind speed in the typhoon-ocean coupled model was weaker than that in the TYM. Besides, sensible and latent heat fluxes decreased mainly around the typhoon center. Moreover, the amount of precipitation near the center of Typhoon Bilis decreased compared with that in the TYM at the same area. These results in the typhoon-ocean coupled model did not contradict the result of Bender et al. (1993).

4. Discussion

We constructed the typhoon-ocean coupled model system composed of the TYM and the MRI mixed layer ocean model. This model realized SST cooling by passage of Typhoon Bilis in the ocean, and

the negative feedback in the atmosphere. However, we will need further improvements, particularly the physical processes, of both models. One of the important physical processes that we should improve is the boundary layer physics in the TYM. Bender et al. (2001) reported that the low level wind in the GFDL Hurricane-ocean coupled model has exhibited a large negative bias and poor pressure wind-relationship, as the model tends to under-predict surface wind speeds for a given central pressure compared with data of GPS sondes. This is due to the lower version of closure schemes of Mellor-Yamada's. Bender et al. (2001) reported that a level 2.5 Mellor-Yamada turbulent closure scheme was a good performance for pressure-wind relationship, although the JMA actually adopt a level 2 Mellor-Yamada turbulent closure scheme. Moreover, it is evident that the reduction to 10m by the Monin-Obukhov formulation is not valid (Bender et al., 2001). It is the reason the TYM-ocean coupled model adopts the lowest level layer as the surface winds.

The other problem is the interface process between the atmosphere and the ocean. The MRI mixed layer ocean model only adopts the sensible and latent heat fluxes (Bender et al., 1993), and solar insolation and long-wave radiative fluxes are neglected. We try to improve the process of sea surface heat fluxes using diurnal cycling algorithm.

References

Bender, M. A., I. Ginis, and Y. Kurihara 1993:Numerical simulations of the tropical cyclone-ocean interaction with a high-resolution coupled model. J. Geophys. Res., 98, 23245-23263.

Bender, M. A., I. Ginis, T. P. Marchok, and R. E. Tuleya 2001:Changes to the GFDL Hurricane Forecast System for 2001 Including Implementation of the GFDL/URI Hurricane-Ocean Coupled Model. http.//www.gfdl.noaa.gov/~mb/tpd_gfdl.html

Wada, A 2002: The processes of SST cooling by typhoon passage and case study of Typhoon Rex. Pap. Meteor. Geophys. accepted.

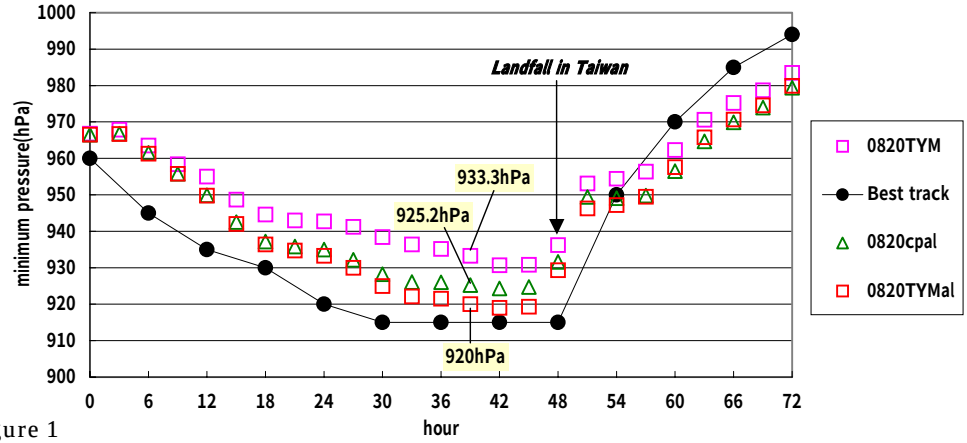

Figure 1
Time series about the intensity forecast of Typhoon Bilis. Horizontal axis represents hours and vertical axis indicates the minimum pressure of Typhoon Bilis.

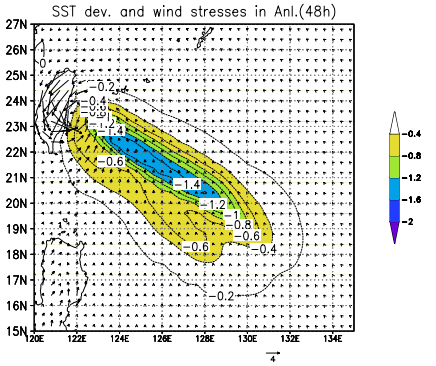

Figure 2
Horizontal SST deviations from the initial time(T+0h) to T+48h. Contour lines and shades show the SST deviation. Vectors show the distribution of wind stresses

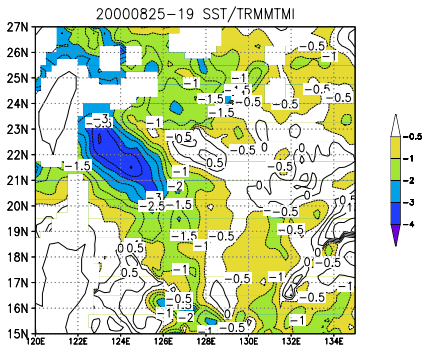

Figure 3
Horizontal SST deviations from August 19, 1998 to August 25, 1998. 'TMISST (Ver. 2.0)' was produced and supplied by the Earth Observation Research Center, National Space Development Agency of Japan."